



## Turbulence measurements with a tethered balloon

CANUT Guylaine<sup>1</sup>, COUVREUX Fleur<sup>1</sup>, LOTHON Marie<sup>2</sup>, LEGAIN Dominique<sup>1</sup>, PIGUET Bruno<sup>1</sup>, LAMPERT Astrid<sup>3</sup>, and MOULIN Eric<sup>1</sup>

<sup>1</sup>CNRM-GAME (Météo-France and CNRS), Toulouse, France

<sup>2</sup>Laboratoire d'Aérodynamique, University of Toulouse, CNRS, France

<sup>3</sup>Institute of Flight Guidance, TU Braunschweig, Hermann-Blenk-Str. 27, 38108 Braunschweig, Germany

Correspondence to: CANUT Guylaine  
(guytaine.canut@meteo.fr)

### Abstract.

This study presents the first deployment of a turbulence probe below a tethered balloon in field campaigns. This system allows to measure turbulent temperature fluxes, momentum fluxes as well as turbulent kinetic energy in the lower part of the boundary layer. It is composed of a sonic thermoanemometer and inertial motion sensor. It has been validated during three campaigns with different convective boundary-layer conditions using turbulent measurements from atmospheric towers and aircraft.

**Keywords.** Boundary layer, turbulence measurements, tethered balloon

### 1 Introduction

The atmospheric boundary layer (ABL) is the lowest part of the atmosphere and hosts turbulent processes responsible for transfer of heat, moisture and momentum between the surface and the free troposphere. The time evolution of the parameters close to the surface is controlled by those turbulent processes. Also the coupling to the surface (either land or ocean) strongly depends on the boundary-layer processes. So, a precise understanding of those processes and in particular of the vertical profiles of turbulent fluxes is crucial to our ability to quantitatively describe and model the evolution of the lower part of the atmosphere and the corresponding energy budget, which are necessary for numerical weather and climate predictions. In recent years, dynamics and lower layers exchange of energy and trace species at the surface / atmosphere interface were studied during national and international programs (SHEBA (Ullrich et al. (2002)), IHOP

(Weckwerth et al. (2004)), AMMA (Lebel et al. (2007)), COPS (Wulfmeyer et al. (2008))).

Understanding the turbulent processes in the ABL requires the knowledge of the evolution of the profile of the sensible heat flux. However, it remains difficult to measure. The observation of these processes raises specific problems because the phenomena involve fine temporal (a few tenths of a second to a few minutes) and spatial scales (of the order of meters to tens of meters). If rapid sensors are available at the ground for most variables (temperature, humidity, wind), in altitude the high-frequency measurements are limited, and the turbulent instruments are mounted mainly on research aircrafts. Previous studies (Lenschow and Stankov (1986), Saïd et al. (2010)) used instrumented aircraft to measure turbulent heat flux in altitude. This platform does not allow to obtain vertical profiles, but only provides some measurements at discrete vertical levels. Usually a linear interpolation of data is used to obtain a profile and estimate fluxes at surface and at the top of ABL. Another inconvenient of aircraft platform is the cost. Recently, studies with remotely piloted aircraft systems (RPAS) (Martin et al. (2014)) show the capability of these small and light platform to measure turbulent heat fluxes in altitude. Fixed-point measurements on tall towers have provided significant insight into the heat fluxes characteristics well above the surface layer (Kaimal et al. (1976); Angevine et al. (1998)) but towers are limited in height with only a few towers worldwide reaching more than 100m. Towers with heights exceeding 50 m are practically non-portable, which makes them inappropriate for deployment in a field campaign. The logistical limitations of other platforms can partly be overcome by using tethered balloons. This platform offers the potential of a fixed mast but can be used to heights up to 1000m and is easily deployed



2

from various locations. Past studies have used this platform since the 1970s. (Morris et al. (1975); Kaimal et al. (1976);  
10 Ogawa and Ohara (1982); Muschinski et al. (2001)) but this platform has mainly be used to study mean thermodynamical measurements. Lapworth and Mason (1988) developed a system with a turbulence probe composed with a Gill propeller anemometer attached to the tethering cable of a balloon. The  
15 authors used inclinometers and magnetometers to determine the probe sensor orientation. The system weighted around 10kg.

A detailed examination of the general applicability of an instrumented balloon for measuring ABL turbulent fluxes has not been undertaken previously. The objective of this study is to demonstrate that an instrumented balloon can be used for measurements of the heat flux and turbulence structure of the ABL. The major advantage of tethered balloon is the potential to provide flux measurements at various vertical heights  
25 covering a part of the vertical extent of the boundary layer. The turbulence tethered sonde presented here is designed to measure turbulence and sensible heat fluxes. The paper is structured as follows. First we describe the general architecture of the system, the sensor characteristics and the motion correction. Sections 3 and 4 are dedicated to the validation  
30 respectively close to the surface and within the boundary layer using conventional data from towers and aircraft. In section 5, we explore the capability of the system to study the turbulence structure in the framework of the late afternoon transition. Conclusion ends the paper.

## 10 2 Overview of the system

This part describes the general architecture of the system, i.e. the balloon used and the turbulence sonde. The motivation is to develop a simple device that can be easily deployed in different field campaigns. The platform combines slow and  
15 fast sensors to quantify mean and turbulent processes.

### 2.1 Sensor characteristics

In this study we have used the Vaisala 7 m<sup>3</sup> tethered balloon inflated with helium. The model is Vaisala TTB327 (L  
15 4.6 m x H 1.84 m x l 1.84 m 3.1 kg). The balloon is a zeppelin shaped aerostat and it is restrained by a cable attached to the ground (the weight of the cable is 0.5 10<sup>-3</sup> kgm<sup>-1</sup>)  
20 with an electric winch which is used to raise and lower the balloon. The maximum height of flights that can be reached depends on atmospheric conditions (wind speed). We have never tested an altitude higher 1000 m. The turbulence tethered sonde (denoted TS in the following) can be attached to a  
25 wide variety of balloon; a dedicated balloon is not necessary. The instrument package consists of both a slow measurement instrument, a 1Hz vaisala tethered sonde (TTS111 model) mounted below the tethered line as well as fast measurement instrument, called the TS and suspended 8 m below the bal-  
30

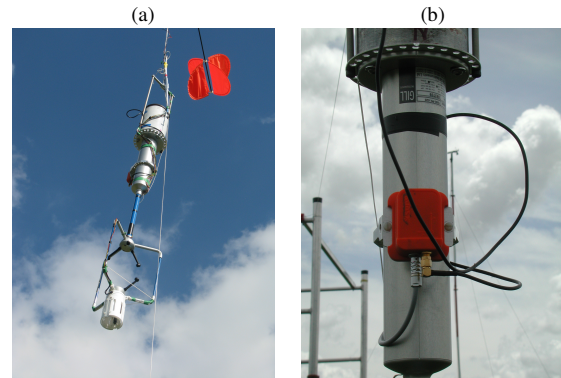


**Figure 1.** Image of the turbulence tethered sonde: (a) The sonic anemometer and the electronic system; (b) the inertial motion sensor.

loon to avoid wind flow distortion due to the balloon. The TS is attached to the cable with an horizontal pivot. The advantage is to limit yaw movements of the TS. The 1Hz vaisala commercial probe provides slow measurements of temperature, humidity, pressure, wind speed and direction, and is able to transmit 1Hz data to the ground using a radio link. This probe is mainly used to monitor the wind in real-time at flight altitude. We have a security constraint given by the balloon manufacturer, in case of wind greater than 12 m s<sup>-1</sup>,  
5 when the flight should be interrupted.

The TS is based on a commercial sonic anemometer (Gill windmasterpro model, fig. 1(a)) which provides measurements of three-dimensional wind and sonic-temperature at 10 Hz. The thermo-anemometer allows to connect others sensors to own analog inputs. An off-the-shelf coupled inertial-GPS motion and attitude sensor (Mti-G at 10 Hz from Xsens, fig. 1(b)) was added in order to correct the anemometer movements. A fast-response thin wire allows the measurement of air temperature fluctuations. Also a standard pressure and temperature sensors provide slow reference measurements. Data was logged aboard on two SD cards. A home made data acquisition system (micro controleur PIC24F) read, date, and log thermo-anemometer and inertial navigation system (INS) incoming numerical RS232 signals. The total mass of the system is 2 kg including batteries (0.3 kg). The sonic anemometer represents the half of the mass (1 kg) whereas the GPS-INS weighted only 0.15 kg. A first performance lies in the low weight of the system. Lapworth and Mason (1988) described a balloon borne turbulence probe system with a weight of 10 kg. The decrease in weight was possible by the miniaturization of sensors in recent years. The system can run for 4h powered by eight 1.2V 2700 mA.h NiMH batteries.



## 2.2 Motion correction

The off-the-shelf coupled inertial-GPS motion and attitude sensor is essentially composed of two parts: (1) an inertial navigation system to measure the balloon's position, speed, and attitude relative to the Earth, and (2) a data acquisition system to record all the incoming signals.

A miniature GPS-INS is attached to the platform 40 cm above the sonic anemometer to provide the position, speed, and orientation of the sonic anemometer.

Linear and rotational speeds provided by the INS are used to calculate the speed of the platform in the coordinate system of the sonic anemometer. This means that the wind vector in the platform coordinate system is a simple vector difference between the sonic and GPS-INS velocities:

$$V_{platform} = V_{sonic} - V_{INS} \quad (1)$$

where  $V_{platform}$  is the wind vector in the platform coordinate system,  $V_{INS}$  is the GPS-INS motion vector, and  $V_{sonic}$  is the platform-relative flow vector measured by the sonic anemometer.

The INS measured angles of attitude (rolls, pitch and yaw angles) allow us to rotate the wind vector measured in the platform coordinate system to the meteorological coordinate system. Geo-referenced  $u$ ,  $v$ ,  $w$  wind components are then calculated from the well adopted equations of Lenschow (1986).

## 3 Validation close to the surface

In order to check the validity of the high-frequency measurements obtained by the TS, the measurements are compared with those of a three-dimensional sonic anemometer fixed on masts and installed during three experimental campaigns between 2010 and 2013. Ideally, for direct comparison with fixed point on tower, flying at constant altitude close to the tower is desirable. The horizontal distance between TS and the position of the towers was lower than 200 m. The two first campaigns took place in summer 2010 and 2011 in the BLLAST (Lothon et al. (2014)) experimental site with a tower equipped with three-dimensional sonic anemometers (CSAT, Campbell Scientific Inc, Logan, UT, USA) at 60 m and the third took place at Bourges (France) in a french military site which was equipped with a tower with three-dimensional sonic anemometers (GILL HS 3-axis, Gill Instruments Limited, Lymington, Hampshire, UK) at 30 m. For all the days considered here, the atmospheric conditions were convective and clear sky. Only the campaign in August 2010 in the BLLAST site was entirely dedicated to the validation of the TS. No scientific constraints were therefore imposed. Indeed, during two days, the TS flew at fixed height corresponding to the instrumented level of the mast. For the other two campaigns, the TS did not remain the whole day at the same height. So we only selected measurement periods when the TS was at a similar level as the fixed sonic anemometer.

Globally, the time series recorded during these different campaigns, after motion correction applied, exhibit excellent agreement even with the aforementioned spatial differences between tower and TS. We hereafter denote  $u'$ ,  $v'$ ,  $w'$  and  $\theta'$  the fluctuations in longitudinal wind, transverse wind, vertical wind and potential temperature respectively. Fluctuations  $x'$  of a variable  $x$  are computed as:  $x' = x - \bar{x}$  where  $\bar{x}$  is the mean over a chosen period. An example of the high-frequency measurements of fluctuations of the three-dimensional winds, and potential temperature is shown in figure 2(a) for a thirty-minute sample on 31 august 2010. The two records do not overlap perfectly but this is expected with fast measurements made 200 meters apart. However, the range of the fluctuations of  $u$ ,  $v$ ,  $w$  and  $\theta$  are similar between the TS and the data from the fixed sonic anemometer. The distribution of the fluctuations recorded during 2-hour period at midday are also presented in figure 2(b). Between both instruments a very similar distribution of all the fluctuations is obtained with same shape and amplitude for all the parameters considered here. Figure 2(c) presents a comparison of smoothed power spectra between both systems for 2 hours measurements at midday for wind components and potential temperature. The comparison between the TS spectra and the tower spectra is generally quite good and both spectra show the expected -5/3 slope at higher frequencies.

For those fluctuation measurements at 10 Hz, several 2nd order moments can be determined. The following subsection presents the validation of variances of the three components of the wind, of the temperature and of the turbulent sensible heat flux. For all the data, the eddy correlation method is used.

### 3.1 Variance

The variance is commonly used for studying some thermodynamical parameters in the boundary layer because it allows to characterize the dispersion around mean values and can be linked to the intensity of the turbulence. Figures 3(a) and (b) present the comparison of the variance of vertical velocity and temperature calculated every 20 minutes during 10 hours between the fixed sonic anemometer on the mast and the TS. The dashed line represents the difference in altitude between both instruments. Note that the position of the tethered balloon varies from a few meters to tens of meters because of turbulent motions of the atmosphere. That is why the variation of altitude around 60 meters is greater in the middle of the day, when the convection is the strongest. During the afternoon, when the difference in altitude is often greater than 10 meters, the values in  $\sigma_w^2$  is higher for the TS while the values in  $\sigma_t^2$  is lower for the TS. This is consistent with the behaviour of a convective ABL in which the fluctuations of temperature are larger near the surface while fluctuations of vertical wind are more important in the middle of ABL. Regarding the variances of the horizontal components of the wind (not shown here) no trend is observed between the two



4

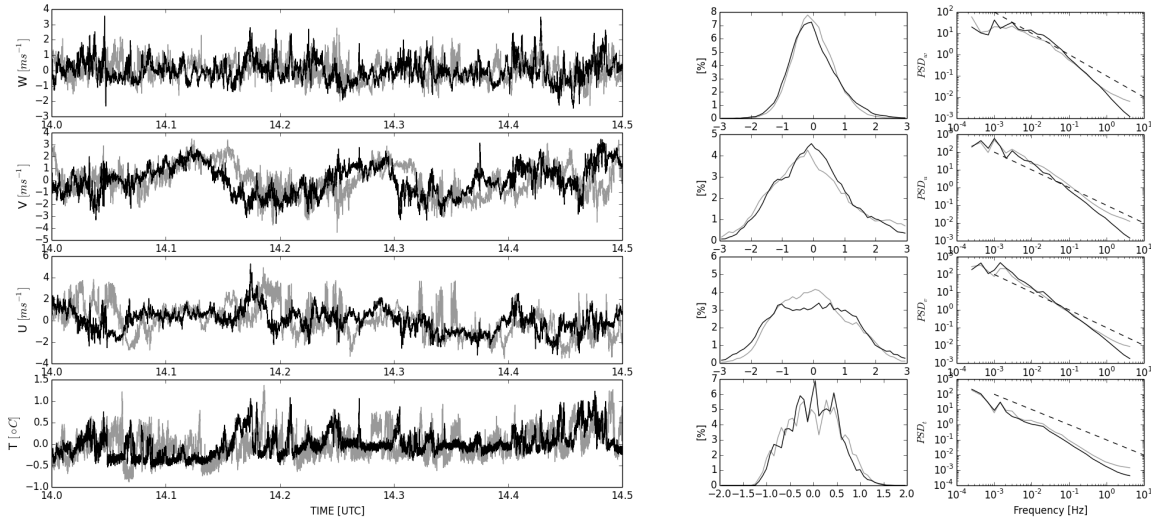


**Figure 2.** Comparison of  $w'$ ,  $v'$ ,  $u'$  and  $\theta'$  measured by a tethered-balloon probe (black) and a sonic anemometer (gray) fixed on a tower nearby for: (left) 10 Hz time series during 30 minute; (middle) fluctuation distribution of a 2-hour sample; (right) power spectra density corresponding to the same sample.

instruments. Usually, when the TS is positioned at exactly the same level as the fixed sonic anemometer, after 1600UTC for the day represented in the figure, the values of the variances obtained are similar between both instruments. Table 1 summarizes the correlation coefficients computed for the different variances measured by both instruments during the three field campaign. For the campaign in Lannemezan in 2010, these correlation coefficients are calculated, based on the data from the 30 and 31 august 2010 between 0800UTC and 2000UTC, i.e. more than 20 hours of data. For  $\sigma_w^2$ ,  $\sigma_v^2$ ,  $\sigma_u^2$  and  $\sigma_\theta^2$  the values are close to unity and confirm the good agreement between both instruments. For the two other campaigns the values are similar than the values obtained in 2010 for all the variance.

### 3.2 Flux

Eddy covariance (Kaimal and Businger (1963), Stull (1988)) is a well established method for the direct measurement of the vertical exchange of gases and/or particles in the atmosphere, suitable for use in a variety of environments. The turbulent flux ( $F_x$ ) is given by the covariance between fluctuations of vertical wind velocity ( $w'$ ) and those of the tracer of interest (noted  $x$  below and represented in this study by potential temperature  $t$ , or horizontal wind component  $u$  and  $v$ ) for the averaging period ( $T_m$ ) such that:

$$F_x = \int_0^T w' x' dt \quad (2)$$

**Table 1.** The correlation coefficient between TS and sonic anemometer on the mast for the variances of the 3 components of the wind, the potential temperature, the sensible heat and the momentum kinematic fluxes.  $r_{2010}^2$  is for the dedicated campaign in 2010 and  $r_{BLLAST}^2$  and  $r_{BOURGES}^2$  correspond to BLLAST and Bourges fields campaigns respectively.

	$\sigma_w^2$	$\sigma_v^2$	$\sigma_u^2$	$\sigma_\theta^2$	$w't'$	$w'u'$	$w'v'$
$r_{2010}^2$	0.88	0.94	0.80	0.84	0.92	0.81	0.80
$r_{BLLAST}^2$	0.85	0.93	0.82	0.84	0.87	0.80	0.76
$r_{BOURGES}^2$	0.90	0.90	0.85	0.80	0.88	0.84	0.82

$F_u$  and  $F_v$  thus denote the momentum fluxes,  $F_\theta$  the buoyancy flux. A measurement frequency of 10Hz and  $T_m = 30$  minutes are generally considered acceptable for tower based instruments to capture the frequency bandwidth of eddy sizes contributing to the flux (Aubinet et al. (2012)). To ensure that the averaging period is long enough we calculate the ogive (not shown here) using the cumulative integral of the spectrum of the turbulent flux starting at the highest frequencies. From these plot, a period greater than 16 minutes is determined as sufficient to calculate the turbulent fluxes. Therefore, in the following, we chose 20 minutes for computing the fluxes with both tower and TS data. Figure 3(c) shows the comparison between the TS and the fixed sonic anemometer for the sensible heat flux during 10 hours of measure-

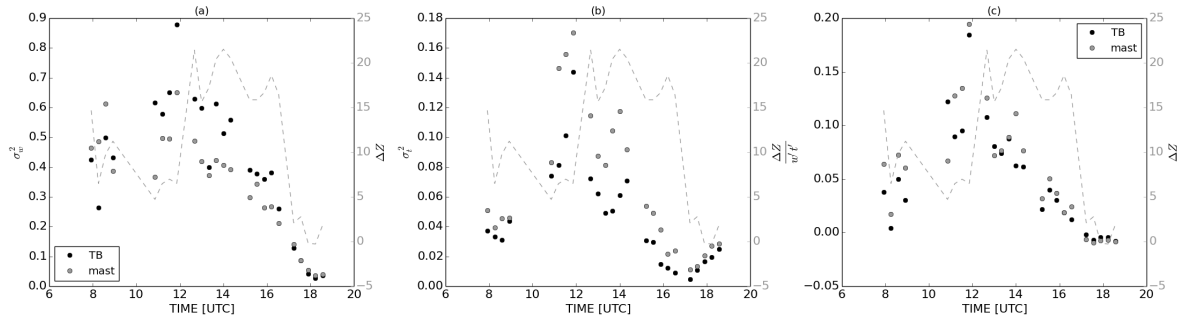


**Figure 3.** Temporal evolution of turbulent moments measured by the tethered balloon (black) and the tower (gray) on 31 August 2010: (a) vertical velocity variance, (b) temperature variance and (c) buoyancy flux. The dashed line represents the variation of the altitude of the tethered balloon) around 60 meters.

ments. The agreement is satisfactory even if  $F_\theta$  seems systematically larger for the tower data during the convective period. This is consistent with TS always positioned above the tower (between ten and twenty meters) and a quasi-linearly vertically decrease of the sensible heat flux in these atmospheric conditions. For that day, correlation coefficients between both datasets is 0.92, 0.81 and 0.8 (Table 1) for  $F_\theta$ ,  $F_u$  and  $F_v$  respectively. More differences are found for  $F_u$  and  $F_v$  than for  $F_\theta$  but one explanation could be that the flow is distorted by the tower (Miller et al. (1999)) and may induce modifications of the fluctuations of zonal and meridional wind. To summarize, Figure 4 presents the comparison of the turbulent sensible heat fluxes between tower and TS observations for the entire set of available data (63 segments of 20 minutes), including selected periods of BLLAST and BOURGES campaigns for which the tethered balloon flight was located at a similar altitude of a sonic anemometer on the tower which for more than 20 minutes. The maximum of altitude difference is 30 meters. The range of data is between 0 and  $0.2 \text{ Kms}^{-1}$ . The coefficient correlation between TS and fixed sonic anemometer for the sensible heat flux parameter is 0.85, indicating a good agreement for different places, moments of the days.

#### 4 Validation within the PBL

In this section, we use data from aircraft and remotely piloted aircraft systems to look at the behaviour of the TS in altitude while the previous section concentrates on the validation of the turbulent data from TS close the surface with fixed sonic anemometers. Among the three campaigns of this study, only the BLLAST field campaign offers complementary data to validate the data of the TS above 60 m. The BLLAST field campaign has been described in details in Lothon et al. (2014). The aim was to understand the turbulent processes during the transition at the end of the afternoon, when the boundary layer turns from convective to residual. This campaign brought together many complementary observation devices including Remotely Piloted Airplane System (RPAS), aircraft, wind profilers, sodar, lidars, tethered balloons and balloon soundings, among others, with the objective of achieving an exhaustive description of the dynamical processes in the boundary layer. The campaign documented 11 days with systematically intensification of the observations during the afternoon. It is in this context that the TS was deployed during the 11 Intensive Observation Periods (IOPs). Table 2 summarizes the duration of the flights of the TS. Most of the time, the flights started at the beginning of the afternoon and ended before 2000UTC. Battery life was not long enough to cover the entire period and the flights were cut in 2 parts. The altitude of the TS is variable according to the different IOPs but remained between 150 and 500 m, corresponding to the

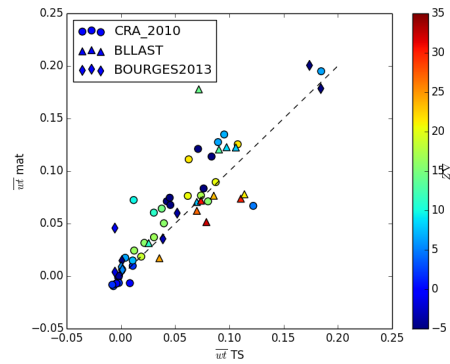


**Figure 4.** Correlation plot between sensible heat flux obtained by TS and data from towers during three different campaigns at two different places in summer 2010, 2011 and 2013. The color corresponds to the altitude difference between TS and sonic anemometer on tower.

to residual. This campaign brought together many complementary observation devices including Remotely Piloted Airplane System (RPAS), aircraft, wind profilers, sodar, lidars, tethered balloons and balloon soundings, among others, with the objective of achieving an exhaustive description of the dynamical processes in the boundary layer. The campaign documented 11 days with systematically intensification of the observations during the afternoon. It is in this context that the TS was deployed during the 11 Intensive Observation Periods (IOPs). Table 2 summarizes the duration of the flights of the TS. Most of the time, the flights started at the beginning of the afternoon and ended before 2000UTC. Battery life was not long enough to cover the entire period and the flights were cut in 2 parts. The altitude of the TS is variable according to the different IOPs but remained between 150 and 500 m, corresponding to the



6

first half of the ABL. The French Piper aztec aircraft from SAFIRE mainly flew in the middle-to-late afternoon and measured pressure, temperature, moisture, CO<sub>2</sub> concentration and 3-D wind with a spatial resolution of 3 m within the ABL (DOI:10.6096/BLLAST.PiperAztec.Turbulence). Flights generally included stacked level runs in vertical planes within the ABL in the region of the instrumental site. M2AV (Martin et al. (2014), Wildmann et al. (2014)) remotely piloted aircraft systems were deployed for four IOPs with also an intensification of flights in the middle-to-late afternoon. M2AV measured at 100 Hz temperature, 3-D wind and humidity at 1 Hz. Flights included straight leg of 1 km length around 300 m of altitude. In this paper, only the M2AV data from the IOP on 02 July 2015 are used.

#### 4.1 The turbulent kinetic energy

The turbulent kinetic energy, noted TKE, is one of the most important variables used to study turbulent boundary layers since it quantifies the intensity of turbulence which controls vertical mixing (Lenschow and Stankov (1974) André et al. (1978) Lenschow and Stephens (1980)). It is defined as:

$$TKE = 0.5(\sigma_w^2 + \sigma_u^2 + \sigma_v^2), \quad (3)$$

and is one of the common parameters measured by TS, aircraft and M2AV. Depending on the different platforms the integrated times to compute TKE could vary. For TS we choose to take 20 minutes as determined by the ogive method (see section 3). For aircraft estimation the calculation is made with data recorded along stacked legs of around 40 km (around 6 minutes). For M2AV we have an estimation for each straight leg of 1 km length (corresponding to 3 minutes). To be consistent with the TS data, an averaging of 20 minutes is applied to the M2AV data. Figure 5 presents the comparison between the three platforms. We selected only the data when the difference in altitude between TS and aircraft or M2AV was smaller than 250 m. In convective conditions, the TKE parameter present quasi constant values in the middle of the ABL and it is the reason why we can compare the TKE observed by the three platforms even if altitudes are not exactly identical. The data set consists of ten different IOPs. The dataset presents a large range of values of TKE between 0 and 1.5  $m^2s^{-2}$ . Most of the time the altitude of the aircraft is above the TS and it is the contrary when we consider the data from M2AV. Here again, the correlation coefficient is close to unity ( $r = 0.88$ ) indicating a good agreement between the three platforms and confirming that the estimation of TKE in altitude by TS is reliable.

#### 4.2 Heat flux

Unlike the TKE, the sensible heat flux observed in a convective boundary layer presents a linear decrease with height and becomes negative close to the boundary-layer top. This feature makes it difficult to compare data from TS and air-

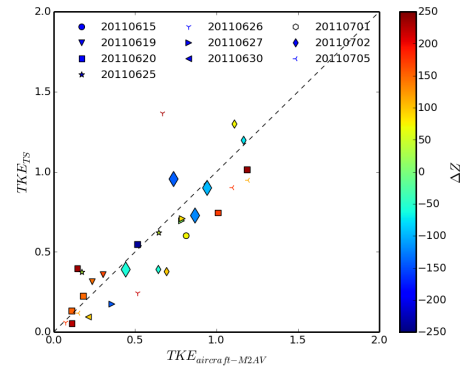


**Figure 5.** Turbulent kinetic energy measured from tethered balloon (y-axis) vs. the one measured by aircraft or M2AV (x-axis) for 10 IOPs during the BLLAST campaign in June/July 2011. Small symbols are used for aircraft and bigger ones are used for M2AV (for 2 July). The color corresponds to the altitude difference between TS and aircraft or M2AV.

craft when their altitudes are not similar. In particular, aircraft flight altitude is often located close to the level where the sign of the heat flux changes making uncertain the flux determination by aircraft. When comparing data from the TS during BLLAST with fixed mast data we systematically see a decrease of the sensible heat flux with altitude. Figure 6 shows an example of the profile of the sensible heat flux obtained in the ABL for 02 July 2011. For two different times, the combination of data from fixed tower, TS and aircraft shows a decrease of the sensible heat flux with altitude. This does not allow us to directly validate the measurement of sensible heat fluxes but at least indicate consistency among the different datasets.

### 5 The Turbulence tethered sonde in the framework of the BLLAST study

As seen in section 4, during the BLLAST campaign, the TS data have been added to a very rich datasets with several levels of instrumented measurements on 60 m tower, aircraft flights and RPAS. In this section we focus more on the evolution of the TKE during the afternoon obtained with TS.

#### 5.1 Turbulent kinetic energy

Figure 7 presents the afternoon evolution of the TKE during the 10 IOPs obtained with aircraft, TS and the tower. Concerning the timing of the decreasing of the TKE, we observe a similar behaviour for all the days. Until 1600UTC, before TKE starts to decrease, it is maintained close to 1 at the surface (sonic anemometer on a tower at 8 m) and also in the middle of the ABL (between 0.2 and 0.6  $z_*$  with aircraft

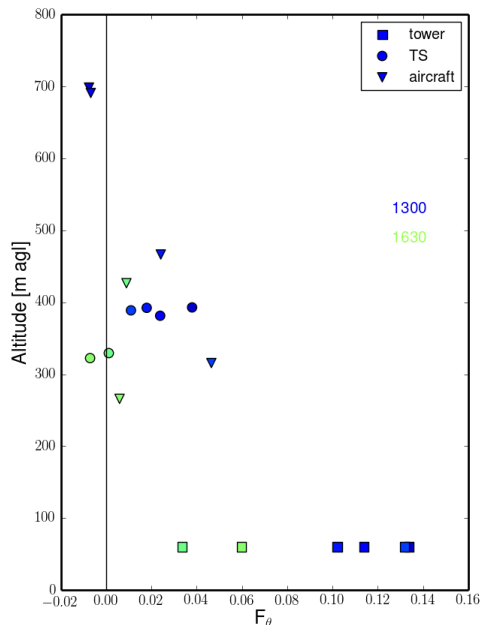


**Figure 6.** Sensible heat flux profiles obtained with (triangle) aircraft, (circle) TS and (square) sonic anemometer on the 60 m tower on 02 July 2011 during the BLLAST field campaign. The color corresponds to the time of the day.

and TS). However, after 1600UTC, when the decay starts, we can see that the value at 8 m remains larger than the TKE observed above until the end of the late afternoon transition. This result is consistent with the results obtained by Darbieu et al. (2015). The authors have shown the existence of 'pre-residual layer' in altitude characterized by a decay of the TKE which is initiated first in altitude.

## 5.2 Anisotropy of the turbulence

One of the issues the BLLAST project focuses on is the vertical structure of the turbulence properties in the boundary layer. In particular, the anisotropy of turbulence is of interest during the afternoon transition (Darbieu et al. (2015), Couvreux et al. (2015)).

Here, to estimate anisotropy, we define the ratio

$$A = \frac{3}{2} \frac{w'^2}{TKE}. \quad (4)$$

It is based on the fact that when the turbulence is isotropic ( $u'^2 = v'^2 = w'^2$ ),  $TKE = 3/2 w'^2$  and  $A = 1$ . The TKE can thus be estimated only from the variance of  $w'$ . When  $A = 3$ , the horizontal contribution to the TKE is zero ( $u'^2 = v'^2 = 0$ )

Day	time of start	time of end	altitude of flight	$z_*$
20110615	1456	1652	200	0.2
	1815	1850	400	0.4
20110619	1315	1550	150	0.1
	1720	2010	500	0.5
20110620	1300	1600	150	0.1
	1645	1950	500	0.5
20110624	1715	1900	250	0.4
20110625	1245	1625	300	0.4
	1700	1945	250	0.5
20110626	1230	1700	350	0.4
	1710	2000	250	0.5
20110627	1330	1600	400	0.4
	1645	1945	350	0.9
20110630	1240	1525	300	0.2
	1620	1950	400	0.2
20110701	1310	1430	200	0.1
	1450	1530	200	0.2
20110702	1230	1530	400	0.4
	1630	1945	350	0.3
20110705	1345	1645	300	0.3
	1730	2000	300	0.3

**Table 2.** Characteristics of the different TS flights;  $z_*$  is the ratio between the altitude and the top of the boundary layer.

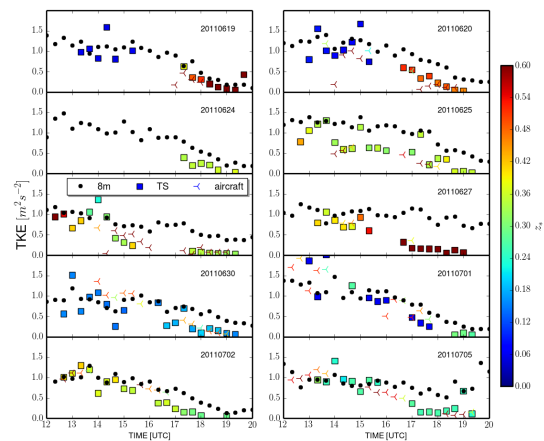


**Figure 7.** Time evolution of the turbulent kinetic energy measured from (□) the turbulence tethered sonde (○), the 8 m tower and the (△) aircraft during 10 IOPs. The color is function of  $z_*$ .

and the turbulence is controlled by vertical motions. When  $A=0$ , the vertical contribution to the TKE is zero ( $w'^2 = 0$ ) and the turbulence is only created by horizontal wind fluctuations.

Figure 8 presents the time evolution of the ratio estimated by equation 4 and calculated by the sonic anemometer at 8 m (Nilsson et al. (2015)) and by the TS higher in altitude (see table 2). For all the IOPs, values are larger at higher altitude



than close the surface. The ratio is larger than 1 which means that the contribution of the horizontal motion is small. At low altitude (8 m on the figure) but also at 30, 45 and 60 m (not shown here) the contribution between horizontal and vertical motion are more equivalent. At the end of the day, the values are similar between measurements in altitude and close the surface. The evolution of the anisotropy ratio obtained with TS is in agreement with the results from Darbieu et al. (2015) obtained with LES models for one IOP of the BLLAST campaign. The authors show also that the contribution of the vertical velocity variance contribute to the TKE is larger in the middle than in the upper and lower parts of the PBL, due to small vertical velocity variance close to the surface and in the entrainment zone and larger shear at the interfaces.

Values of  $A$  show the anisotropy of turbulence in the middle of the ABL in these convective conditions. This is an important issue when for instance one wants to access to the TKE while only  $w'^2$  is measured as for example with a vertically pointing doppler lidar (Gibert et al. (2011)).

This section demonstrates the interest of the observations made by TS which allows continuous exploration of the middle of the boundary layer during the transition phase. Synergy with the other traditional tools (aircraft and tower) allow to study the turbulent processes between the surface and the top of the boundary layer as shown by Figure 6.

## 6 Conclusions

In this paper, a new system to estimate turbulent transfer in the boundary layer as well as the associated first measurements have been presented. It consists in a turbulence probe mounted on a tethered balloon. Those measurements have been evaluated by comparison to turbulent measurements derived from tower, aircraft and remotely piloted aircraft system and show very good consistency with those more traditional turbulence measurements. This new system presents several advantages:

- the turbulence is estimated in the lower part of the PBL at altitudes where the research aircrafts encounter some difficulties to fly.
- with this TS system, measurements in the boundary layer can be made frequently and inexpensively.

The only limitation for the deployment of this platform is that moderate wind ( $<12 \text{ m.s}^{-1}$ ) conditions are required. We demonstrated here that the turbulence sonde is capable of measuring heat and momentum fluxes using the direct eddy-covariance method. For the first time, this new instrumental platform was used to measure heat flux and TKE. It was shown that it is possible to characterize different kinds of vertical motions occurring at the middle of PBL. After this first validation we are considering to explore the possibility to estimate continuous vertical profiles of the dissipation rate of

TKE by maintaining a slow descending rate during the profile and using a moving average over a given time period. Also we would like to load off the system to add a fast humidity sensor such as a krypton KH2O (Campbell Scientific Ltd) to measure turbulent latent heat flux simultaneously with the turbulent sensible heat flux. Another advantage is to deploy the system simultaneously with other instruments (particles counter, O<sub>3</sub>-CO<sub>2</sub> probes, droplets, ...) to better understand the link between microphysics and atmospheric turbulence like for example in fog. The TS can also be used to validate remote sensing turbulence measurement (lidar, radar, sodar).

*Acknowledgements.* The authors thank F. Said for providing the tower measurements. The BLLAST field experiment was made possible thanks to the contribution of several institutions and supports: INSU-CNRS (Institut National des Sciences de l'Univers, Centre National de la Recherche Scientifique, LEFE-IMAGO program), Météo-France, Observatoire Midi-Pyrénées (University of Toulouse), EUFAR (European Facility for Airborne Research), BLLATE-1 & 2, COST ES0802 (European Cooperation in the field of Scientific and Technical). The field experiment would not have occurred without the contribution of all participating European and American research groups, which all have contributed in a significant amount. The Piper Aztec research airplane is operated by SAFIRE, which a unit supported by INSU-France, Météo-France and the French Spatial Agency (CNES). BLLAST field experiment was hosted by the instrumented site of Centre de Recherches Atmosphériques, Lannemezan, France (Observatoire Midi-Pyrénées, Laboratoire d'Aérodynamique).

## References

- André, J. C., De Moor, G., Lacarrere, P., Thery, G., and du Vachat, R.: Modeling the 24-hour evolution of the mean and turbulent structure of the planetary boundary layer, *J. Atmos. Sci.*, 35, 1861–1883, 1978.
- Angevine, W. M., Bakwin, P. S., and Davis, K. J.: Wind profiler and RASS Measurements compared with measurements from a 450-m-tall tower, *J. Atmos. Oceanic Tech.*, 15, 818–825, 1998.
- Aubinet, M., Vesala, T., and Papale, D.: Eddy covariance. A Practical Guide to Measurement and Data Analysis, Edition Springer Atmospheric Science, 2012.
- Couvreur, F., Bazile, E., Canut, G., Seity, Y., Lathon, M., Lohou, F., Guichard, F., and Nilsson, E.: Boundary-layer turbulent processes and mesoscale variability represented by Numerical Weather Prediction models during the BLLAST campaign, *Atmos Chem Phys Dis.*, 2015.
- Darbieu, C., Lohou, F., Lathon, M., Vilà-Guerau de Arellano, J., Couvreur, F., Durand, P., Pino, D., Patton, E. G., Nilsson, E., Blay-Carreras, E., and Gioli, B.: Turbulence vertical structure of the boundary layer during the afternoon transition, *Atmospheric Chemistry and Physics*, 15, 10071–10086, doi:10.5194/acp-15-10071-2015, <http://www.atmos-chem-phys.net/15/10071/2015/>, 2015.
- Gibert, F., Arnault, N., Cuesta, J., plougouven, R., and Flamant, P.: Internal gravity waves convectively forced in the atmospheric

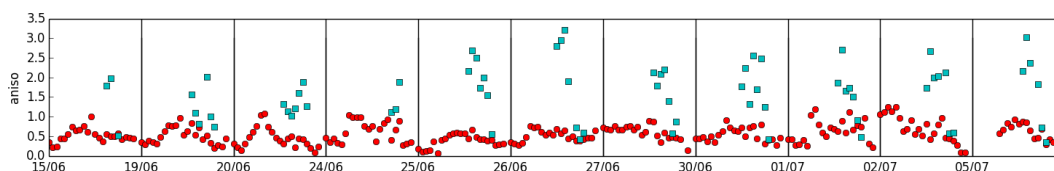


**Figure 8.** Time evolution of the anisotropy ratio measured by tethered balloon (cyan squares) and 8m-tower (red dots).

- residual layer during the morning transition, *Quart. J. Roy. Meteorol. Soc.*, 137, 1610–1624, 2011.
- Kaimal, J. C. and Businger, J. A.: A continuous wave sonic anemometer-thermometer, *J. Clim. Appl Meteorol.*, 2, 156–164, 1963.
- Kaimal, J. C., Wyngaard, J. C., Haugen, D. A., Coté, O. R., and Izumi, Y.: Turbulence structure in the convective boundary layer, *J. Atmos. Sci.*, 33, 2152–2169, 1976.
- Lapworth, A. J. and Mason, P. J.: The New Cardington Balloon-Borne Turbulence Probe System, *J. Atmos. Oceanic Technol.*, 5, 699–714, 1988.
- Lebel, T., Parker, D. J., Bourles, B., Flamant, C., Marticorena, B., Peugeot, C., Gaye, A., Haywood, J., Mougou, E., Polcher, J., Redelsperger, J.-L., and Thorncroft, C.: The AMMA field campaigns: Multiscale and multidisciplinary observations in the West African region, Submitted to *Ann. Geophys.*, 2007.
- Lenschow, D. H.: Aircraft measurements in the boundary layer, *American Meteorological Society*, pp. 39–55, 1986.
- Lenschow, D. H. and Stankov, B. B.: Model of the height variation of the turbulence kinetic energy budget in the unstable planetary boundary layer, *J. Atmos. Sci.*, 31, 465–474, 1974.
- Lenschow, D. H. and Stankov, B. B.: Length scales in the convective boundary layer, *J. Atmos. Sci.*, 43, 1198–1209, 1986.
- Lenschow, D. H. and Stephens, P. L.: The role of thermals in the convective boundary layer, *Boundary-Layer Meteorol.*, 19, 509–532, 1980.
- Lothon, M., Lohou, F., Pino, D., Couvreur, F., Pardyjak, E. R., Reuder, J., Vilà-Guerau de Arellano, J., Durand, P., Hartogensis, O., Legain, D., Augustin, P., Gioli, B., Lenschow, D. H., Faloua, I., Yagüe, C., Alexander, D. C., Angevine, W. M., Bargain, E., Barrié, J., Bazile, E., Bezombes, Y., Blay-Carreras, E., van de Boer, A., Boichard, J. L., Bourdon, A., Butet, A., Campistron, B., de Coster, O., Cuxart, J., Dabas, A., Darbieu, C., Deboudt, K., Delbarre, H., Derrien, S., Flament, P., Fourmentin, M., Garai, A., Gibert, F., Graf, A., Groebner, J., Guichard, F., Jiménez, M. A., Jonassen, M., van den Kroonenberg, A., Magliulo, V., Martin, S., Martínez, D., Mastroiello, L., Moene, A. F., Molinos, F., Moulin, E., Pietersen, H. P., Piguet, B., Pique, E., Román-Cascón, C., Rufin-Soler, C., Saïd, F., Sastre-Marugán, M., Seity, Y., Steeneveld, G. J., Toscano, P., Traullé, O., Tzanos, D., Wacker, S., Wildmann, N., and Zaldei, A.: The BLLAST field experiment: Boundary-Layer Late Afternoon and Sunset Turbulence, *Atmospheric Chemistry and Physics*, 14, 10931–10960, doi:10.5194/acp-14-10931-2014, <http://www.atmos-chem-phys.net/14/10931/2014/>, 2014.
- Martin, S., Beyrich, F., and Bange, J.: Observing Entrainment Processes Using a Small Unmanned Aerial Vehicle: A Feasibility Study, *Boundary-Layer Meteorology*, 150, 449–467, doi:10.1007/s10546-013-9880-4, 2014.
- Miller, D., Tong, C., and Wyngaard, J.: The Effects of Probe-Induced Flow Distortion on Velocity Covariances: Field Observations, *Boundary-Layer Meteorology*, 91, 483–493, doi:10.1023/A:1001868030313, 1999.
- Morris, A. L., Call, D., and McBeth, R. B.: A small tethered balloon sounding system, *Bull. Amer. Meteor. Soc.*, 56, 964–969, 1975.
- Muschinski, A., Frehlich, R., Jensen, M., Hugo, R., Hoff, A., Eaton, F., and Balsley, B.: Fine-Scale Measurements Of Turbulence In The Lower Troposphere: An Intercomparison Between A Kite- And Balloon-Borne, And A Helicopter-Borne Measurement System, *Boundary-Layer Meteorology*, 98, 219–250, doi:10.1023/A:1026520618624, <http://dx.doi.org/10.1023/A%3A1026520618624>, 2001.
- Nilsson, E., Lothon, M., Lohou, F., Pardyjak, E., Mahrt, L., and Darbieu, C.: Turbulence kinetic energy budget during the Afternoon transition, Part A: Observed surface the budget and boundary layer description for 10 Intensive Observation Period Days, *Atmos Chem Phys Dis.*, 2015.
- Ogawa, Y. and Ohara, T.: Observation of the turbulent structure in the planetary boundary layer with a Kyttoon-Mounted ultrasonic anemometer system, *Boundary-Layer Meteorol.*, 22, 123–131, 1982.
- Saïd, F., Canut, G., Durand, P., Lothon, M., and Lohou, F.: Seasonal evolution of boundary-layer turbulence measured by aircraft during the AMMA 2006 Special Observation Period, *Quart. J. Roy. Meteorol. Soc.*, 136, 47–65, 2010.
- Stull, R. B.: An introduction to Boundary Layer Meteorology, vol. new edition 1999, Kluwer Academic Publishers, 666 pp, 1988.
- Utall, T. and al.: Surface heat budget of the arctic ocean, *Bull. Amer. Meteor. Soc.*, 83, 225–275, 2002.
- Weckwerth, T., Parsons, D. B., Koch, S. E., Moore, J. A., Demoz, B. B., Flamant, C., Geers, B., Wang, J., and Feltz, W. F.: An overview of the international H20 project (IHOP\_2002) and some preliminary highlights, *Bull. Amer. Meteorol. Soc.*, 85, 253–277, 2004.
- Wildmann, N., Ravi, S., and Bange, J.: Towards higher accuracy and better frequency response with standard multi-hole probes in turbulence measurement with remotely piloted aircraft (RPA), *Atmospheric Measurement Techniques*, 7, 1027–1041, doi:10.5194/amt-7-1027-2014, <http://www.atmos-meas-tech.net/7/1027/2014/>, 2014.
- Wulfmeyer, V., Behrendt, A., Bauer, H., Kottmeier, C., Corsmeier, U., Blyth, A., Craig, G., Schumann, U., Hagen, M., Crewell, S., Di Girolamo, P., Flamant, C., Miller, M., Montani, A., Mobbs, S., Richard, E., Rotach, M., Arpagaus, M., Russchenberg, H., Schlüssel, P., König, M., Gärtner, V., Steinacker, R., Dorninger, M., Turner, D., Weckwerth, T., Hense, A., and Simmer, C.: The Convective and Orographically-induced Precipitation Study: A Research and Development Project of the World Weather Re-



10

search Program for improving quantitative precipitation forecasting in low-mountain regions., Bull. Amer. Meteor. Soc., 89, 1477–1486, 2008. <sup>645</sup>